Journal of Magnetic Resonance 267 (2016) 30–36

Contents lists available at ScienceDirect

Journal of Magnetic Resonance

journal homepage: www.elsevier.com/locate/jmr

Towards Overhauser DNP in supercritical CO_2

S.G.J. van Meerten, M.C.D. Tayler, A.P.M. Kentgens, P.J.M. van Bentum *

Radboud University, Institute for Molecules and Materials, Heyendaalseweg 135, 6525AJ Nijmegen, The Netherlands

ARTICLE INFO

Article history:
Received 24 February 2016
Revised 1 April 2016
Accepted 3 April 2016
Available online 6 April 2016

Keywords:
Overhauser
Dynamic Nuclear Polarization
CO_2
Supercritical

ABSTRACT

Overhauser Dynamic Nuclear Polarization (ODNP) is a well known technique to improve NMR sensitivity in the liquid state, where the large polarization of an electron spin is transferred to a nucleus of interest by cross-relaxation. The efficiency of the Overhauser mechanism for dipolar interactions depends critically on fast local translational dynamics at the timescale of the inverse electron Larmor frequency. The maximum polarization enhancement that can be achieved for ^1H at high magnetic fields benefits from a low viscosity solvent. In this paper we investigate the option to use supercritical CO_2 as a solvent for Overhauser DNP. We have investigated the diffusion constants and longitudinal nuclear relaxation rates of toluene in high pressure CO_2. The change in ^1H T_1 by addition of TEMPO radical was analyzed to determine the Overhauser cross-relaxation in such a mixture, and is compared with calculations based on the Force Free Hard Sphere (FFHS) model. By analyzing the relaxation data within this model we find translational correlation times in the range of 2–4 ps, depending on temperature, pressure and toluene concentration. Such short correlation times may be instrumental for future Overhauser DNP applications at high magnetic fields, as are commonly used in NMR. Preliminary DNP experiments have been performed at 3.4 T on high pressure superheated water and model systems such as toluene in high pressure CO_2.

1. Introduction

Nuclear Magnetic Resonance is a versatile tool which is used in a range of different fields, such as: structure elucidation, dynamical studies, metabolomics, and protein studies. The main limitation of NMR is the inherent low sensitivity.

In 1953 Albert Overhauser proposed a method to transfer polarization from electron spins to nuclear spins [1]. Since the gyromagnetic ratio of an electron is orders of magnitude larger than that of a nuclear spin this method can be used to improve NMR sensitivity. This method was first demonstrated experimentally by Carver and Slichter [2] for NMR in metals and by Abragam for a liquid containing paramagnetic impurities [3]. In the past decade interest in Overhauser DNP has re-emerged with the aim to implement it at the high magnetic fields that are now common in NMR spectroscopy. Successful pilot studies have been performed at 144 MHz [4,5] and 400 MHz [6,7].

The efficiency of the Overhauser DNP cross-relaxation depends on the fluctuations in the interaction between an unpaired electron spin and a nuclear spin. In liquids these fluctuations are mainly caused by molecular translational motions. Overhauser DNP becomes efficient when the correlation time of the fluctuations is shorter than the inverse electron Larmor frequency ($\tau_c < 1/\omega_e$). At low magnetic fields this condition is satisfied for common solvents, but at high magnetic fields the Overhauser enhancements decrease because the translational dynamics are limited by the viscosity of the solvent.

There have been different approaches to overcome this issue. For example, in a shuttle experiment low field DNP enhancement can be combined with high field NMR detection [8–10]. Another method is to freeze the sample and use solid state DNP methods to transfer polarization. To obtain the high resolution of liquid state NMR the sample has to be either dissolved in a hot liquid [11], or in the case of small volumes the sample can be melted rapidly [12]. For in situ ODNP one can increase solvent mobility by increasing the temperature of the sample [13,7].

In this paper we explore the possibility to extend Overhauser DNP enhancements to higher magnetic field by using supercritical CO_2 ($scCO_2$) as a solvent. The low viscosity of supercritical CO_2 allows for fast molecular motions and short correlation times of the dynamic electron-nuclear dipolar interaction.

Using $scCO_2$ as a solvent for NMR is not a new concept [14,15], and the fast dynamics of molecules in supercritical fluids can be used to reduce the linewidth of quadrupolar nuclei [16]. Also, NMR has been used to monitor the output of Supercritical Fluid

* Corresponding author.
E-mail address: J.vanBentum@science.ru.nl (P.J.M. van Bentum).

http://dx.doi.org/10.1016/j.jmr.2016.04.002
1090-7807/

Chromatography (SFC) and Supercritical Fluid Extractions [17] (SFE). Overhauser DNP in CO_2 solvent was demonstrated for both ^1H and ^{13}C at 0.33 T [18]. In our lab a hyphenation between a modern type of Supercritical Fluid Chromatography (SFC) and NMR has been developed [19]. This SFC-NMR system makes it possible to mix samples with high pressure CO_2 followed by NMR detection. The SFC-NMR is fully automated, which makes it a convenient platform to investigate the influence of various experimental parameters for liquid state Overhauser DNP. A combination of diffusion and relaxation measurements were used to investigate the local dynamics of toluene molecules in CO_2, which can be used to predict the Overhauser enhancements of such a mixture.

The Overhauser DNP mechanism can best be illustrated by considering the relaxation between the energy levels of a coupled two spin system, as reproduced in Fig. 1.

Overhauser DNP is performed by applying microwave radiation at the frequency of the electron transition. This drives the electron spin populations out of thermal equilibrium. Fluctuations in the dipolar interaction between the two spins will induce zero- and double-quantum cross-relaxation, where the dominant double-quantum term induces a negative nuclear polarization [20]. The strength of the cross-relaxation, induced by fluctuating dipolar interactions, can be described by a suitable spectral density function $j(\omega, \tau_c)$, depending on the energy $\omega_e \pm \omega_n$ and correlation time τ_c. In many cases the spectral density function can be approximated by a Force Free Hard Sphere (FFHS) model [21]. In the FFHS model the correlation time is defined as $\tau_c = d^2/(D_S + D_I)$, where D_S and D_I are the diffusion coefficients of the radical and the solute molecules for a given solvent and d is the effective distance of closest approach between the two spins. The FFHS spectral density function drops sharply for $\omega\tau_c > 1$ and Overhauser DNP becomes less efficient at high magnetic fields.

In practice, it turns out that the effective distance of closest approach d is a phenomenological parameter that is specific for a given radical molecule. The potential Overhauser DNP enhancement can be predicted quantitatively for a given solvent if the diffusion constants and d parameter are known. This was for example verified for normal solvents such as water [5] and ethanol [13]. A suitable method is to determine the total longitudinal relaxation as function of the radical concentration. If the (temperature-dependent) diffusion constants are known, the relaxivity can be used to verify the model and to determine the d parameter. Both relaxation and DNP enhancement can then be predicted quantitatively for arbitrary temperature and radical concentration without adjustable parameters. In this paper we will evaluate the validity of this concept for high pressure solvents such as CO_2 with varying toluene content, and doped with TEMPO radicals. This will allow us to predict the potential for future high field Overhauser DNP in supercritical solvents.

The main motivation is that a supercritical fluid can have a density similar to a liquid, while the viscosity is more similar to a gas. CO_2 has no static dipole moment, which is advantageous for DNP because of the reduced dielectric heating of the sample. Even though CO_2 is a non-polar solvent, the addition of a small amount of polar co-solvent, like methanol, increases the solubility of polar solutes drastically [22,23]. For DNP applications, this may also facilitate the use of a variety of radicals.

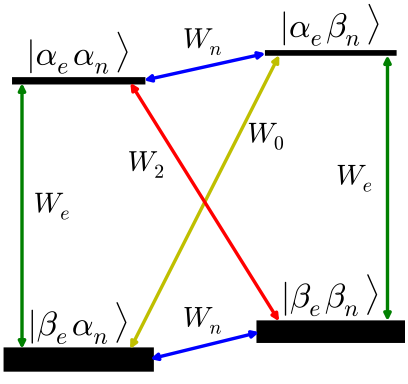

Fig. 1. The energy level diagram of a two-spin system of a coupled electron and nuclear spin. The single quantum relaxation rates are represented by (W_e) and (W_n) for the electron and nuclear spins. The cross-relaxation has two channels, a zero quantum transition (W_0) and a double quantum transition (W_2).

2. Experimental

2.1. Experimental setup

A Waters UPC^2 was modified to create supercritical CO_2 mixtures, which is in-line coupled with the NMR spectrometer. A diagram of the SFC-NMR system is shown in Fig. 2. This setup makes it possible to perform regular supercritical fluid chromatography and interrogate the separated compounds using NMR. The Binary Solvent Manager of the UPC^2 provides the possibility to mix samples into CO_2 in an adjustable volume ratio. The column of the UPC^2 was bypassed to allow direct access of a flow control system to the mixtures generated by the Binary Solvent Manager.

The flow control system is connected in between the UV detector of the chromatograph and the back-pressure regulator (BPR). This flow control system consists of two high-pressure valves (Vici Valco Inc.) operated by an Arduino UNO micro-controller. A schematic of the flow control system is shown in Fig. 3. Valve #1 is used to fill a sample loop of 120 µl with the CO_2 mixture. At a flowrate of 1.5 ml/min the sample loop is filled in approximately 5 s. When this valve is returned to its original position the sample loop is inserted into a flow line of water. The flow of high pressure water, provided by a HPLC pump, keeps the CO_2 at the pressure set by the back-pressure regulator and transports the plug of CO_2 into a 600 MHz Varian NMR spectrometer. A water flow of 0.2 ml/min transports the sample plug to the NMR in 2–3 min. The pressure is monitored during flow with a typical pressure-drop over the flow-line through the NMR probe of about 6 bar. When the CO_2 plug reaches the detection area of the NMR probe valve #2 is

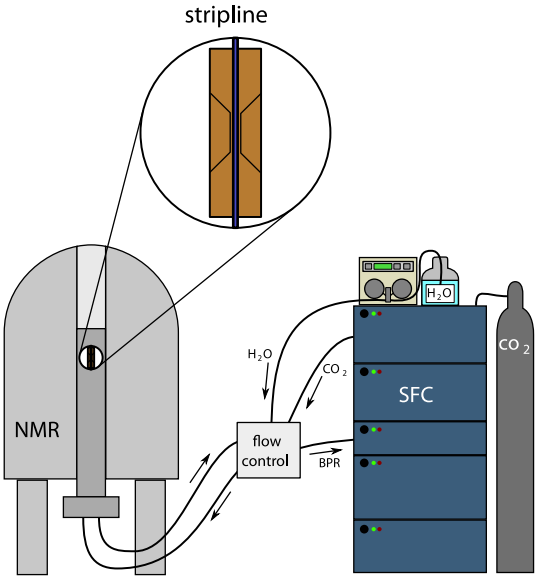

Fig. 2. A diagram of the SFC-NMR setup.

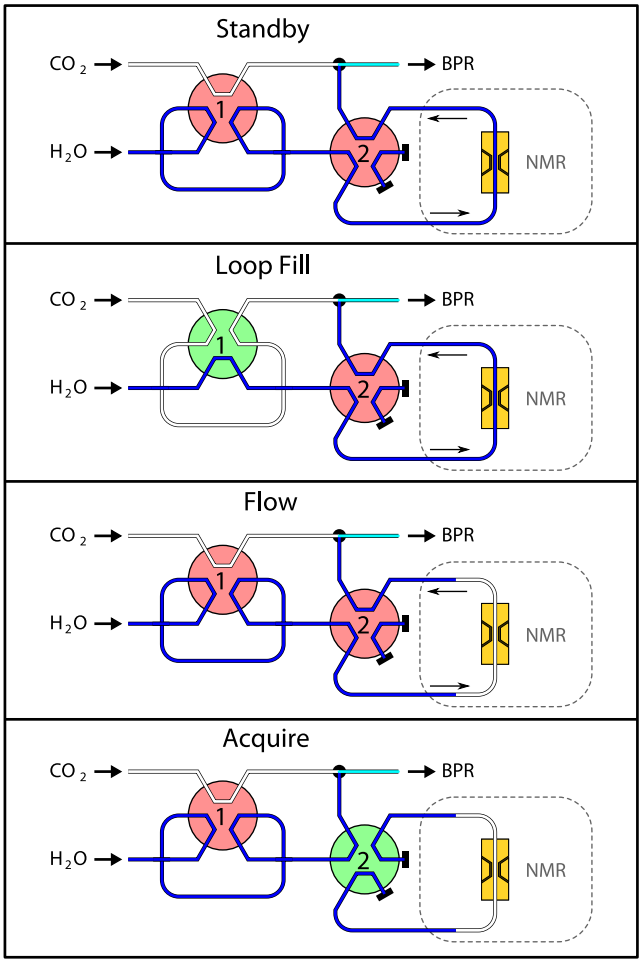

Fig. 3. A diagram of the control system in the various stages of the measurement.

switched. This stops the sample from moving and keeps it at pressure for several hours, which makes it possible to perform long NMR experiments. The Arduino micro-controller then triggers the NMR spectrometer to perform a predefined experiment and store the data after completion. The entire process of sample injection and NMR detection can be repeated and certain parameters, such as volume ratio or temperature, adjusted. This fully automated system can be used to efficiently investigate the effects of a large number of parameters on the properties of high-pressure CO_2.

The NMR detection is performed using a stripline probe [24] with a detection volume of 150 nl. In this design the CO_2 plug is contained in a fused-silica capillary (PolyMicro Technologies) with an outer diameter of 350 μm and an inner diameter of 250 μm. The thin wall of the capillary results in a good filling factor of the stripline, while being compatible with high pressures (typically 100–300 bar). A hydrophobic capillary (methyl deactivated) was used to prevent water adhesion on the capillary wall.

For our investigation into the local dynamics in CO_2 toluene was chosen as a sample molecule. The diffusion constant of toluene in toluene–CO_2 mixtures has been determined using a B_1-field gradient method [25]. The B_1-field gradient was created by using a tapered stripline design [26]. Applying a hard rf-pulse to a tapered stripline creates an amplitude encoding along the B_0-field axis. After a mixing period in the order of 1 s an rf-pulse is used to read out the magnetization. Increasing the power or length of the encoding pulses results in a Gaussian decrease in signal intensity similar to the more common pulsed field gradient methods [27].

The T_1 relaxation times of the methyl and the ring hydrogens of toluene in CO_2 were determined using saturation recovery experiments. The measurement was repeated with increasing concentrations of TEMPO free radical added to the mixture. The correlation time of the electron-nuclear dipolar interaction was determined for mixtures at different temperatures. Also the effect of co-solvent concentration was investigated by varying the toluene content in CO_2.

Preliminary DNP experiments were performed at a 3.4 T magnet using a double resonance probe [28]. The probe consist of a non-radiative dielectric resonator. The microwave mode structure of such a resonator is comparable to that of a metallic cylindrical TE011 resonator. The open structure makes it easier to couple the resonator to a single mode waveguide and simplifies the construction. Most important is the fact that the dielectric material reduces the size of the resonator and thus provides a stronger conversion factor (higher microwave B_1 field amplitude per unit power of radiation). The NMR detection is performed using a small coil located in the center of the microwave resonator. The sample is contained in a fused quartz capillary with 200 μm outer and 100 μm inner diameter. The capillary is connected to the flow setup as shown in Fig. 3. Microwaves were generated using a diode multiplier system driven by a variable frequency synthesizer (VDI). The maximum power output of the digital tunable oscillator is 250 mW near the center frequency of 95 GHz. The output of the oscillator is amplified by an Extended Interaction Klystron amplifier (CPI Canada, VKB2463) that is capable of generating 100 W microwave power. For the liquid state DNP experiments a maximum power of 5 W is needed. The NMR acquisition was performed using a Varian Infinity Plus spectrometer.

3. Results

3.1. Toluene diffusion in CO_2

The effect of toluene content on the dynamics in the CO_2 mixture was investigated by measuring the room temperature diffusion coefficient of toluene in CO_2 at various concentrations. The self-diffusion coefficient of pure toluene is known (2.3×10^{-9} m^2/s) and is used as a reference in the diffusion experiment. The results for the diffusion constant as function of the molar fraction of toluene in CO_2 are shown in Fig. 4.

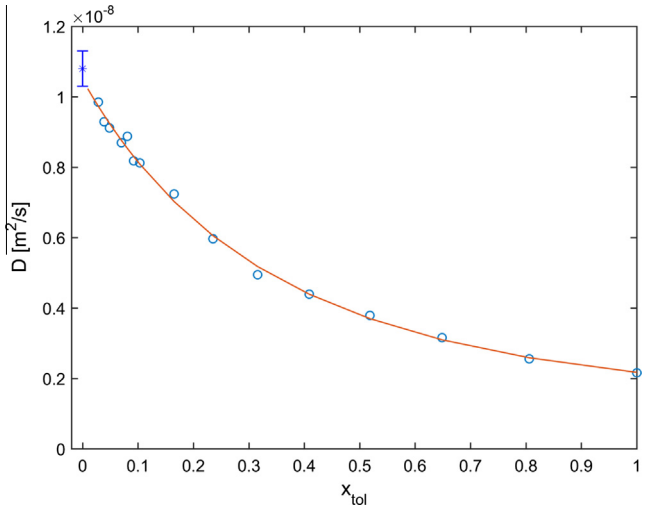

Fig. 4. The diffusion constants of toluene in a toluene–CO_2 mixture determined using a B_1-field gradient method (107 ± 3 bar, 18.0 ± 0.5 °C).

The diffusion curve shows a slow increase as the toluene concentration in CO_2 is reduced. In the limit for very low toluene concentration, the diffusion constant increases rapidly to about 1.1×10^{-8} m^2/s at 18 °C. The diffusion constant of TEMPO in toluene is unknown, but can be estimated from the viscosity of the solvent, using the Stokes–Einstein equation. For example, the diffusion constant of TEMPO in *n*-hexane is known experimentally [29] and can be used as a reference. The viscosity of *n*-hexane is 0.30 mPas (at 25 °C) and the viscosity of toluene is 0.56 mPas (at 25 °C) [30]. Using the Stokes–Einstein relation and a diffusion constant of toluene in *n*-hexane [31] of 4.13×10^{-9} m^2/s, we obtain a self-diffusion constant for toluene of 2.2×10^{-9} m^2/s, consistent with the experimental value of 2.3×10^{-9} m^2/s [32]. A similar estimate based on the diffusion constant for TEMPO in *n*-hexane [29] of 2.93×10^{-9} m^2/s yields a predicted diffusion coefficient for TEMPO in pure toluene of 1.6×10^{-9} m^2/s. For the diffusion constant of TEMPO in a toluene–CO_2 mixture we will assume that this will follow the same behavior as measured for toluene in this mixture, scaled to the reference at 100% toluene. Experimental data for the diffusion constant of toluene in CO_2 in the low concentration limit was measured previously as a function of pressure and temperature [33]. If we assume that the diffusion constant scales inversely with the viscosity, it is possible to extrapolate the data to the present regime (20 °C, 107 bar). This estimate is indicated by the blue errorbar at the vertical axis, and agrees well with our data. Note that the temperature of 20 °C is below the critical temperature and the mixture is in the liquid phase. In the supercritical phase, we expect a decrease in density and a further increase of the diffusion constants.

3.2. Overhauser relaxivity

Within the hard-sphere model for translational dynamics, the Overhauser cross-relaxation and the DNP enhancements are fully determined by the diffusion constants and the minimum distance parameter *d*. It is expected that this effective *d* parameter is determined mostly by the molecular structure of the radical and is independent of the solvent as long as the isotropic approximation is valid. A rather stringent test of the model is that the longitudinal relaxation at a given radical concentration can be predicted from the measured diffusion constants using a single phenomenological value for *d* and no other free parameters. The longitudinal relaxation rate for an interacting spin system as shown in Fig. 1 is given by $R_1 = 1/T_1 = W_0 + 2W_1 + W_2 + W^0$, where W_0, W_1 and W_2 are the zero, single and double quantum transition rates respectively and W^0 is the relaxation rate of the molecule in the absence of the radical. To determine W^0 the T_1^0 values of toluene hydrogens in mixtures with various toluene to CO_2 ratios were measured before adding radicals. The room temperature T_1^0 times of the methyl and the ring hydrogens as a function of the molar ratio are shown in Fig. 5(a). At low concentrations the T_1^0 relaxation time of the ring hydrogens approaches 2 min. At low concentrations the average distance between toluene molecules increases, which decreases the intermolecular interactions. For methyl hydrogens on the other hand spin rotation dominates the relaxation. These rather long T_1^0 values are promising for future Overhauser DNP applications, since even at low radical concentrations, the paramagnetic (cross) relaxation will dominate and a leakage factor $f = 1$ ($T_1 \ll T_1^0$) can be realized without compromising the spectral resolution.

To verify the Overhauser model various concentrations of TEMPO were added to a sample of 0.76 M toluene in CO_2 ($x_{toluene} = 0.038$). The relaxation rates as a function of radical concentration are shown in Fig. 5(b). It is clear that even for a concentration of a few mM TEMPO the cross-relaxation dominates the longitudinal relaxation of CH hydrogens. For CH_3 hydrogens, this limit is reached at concentrations above 10 mM. Within the framework of the Overhauser FFHS model, one expects indeed a linear increase of the relaxation rate as function of the radical doping, where the slope is determined by the correlation time τ_c and the distance of closest approach *d*. If the diffusion constants for both radical and solute molecules are known, then *d* is the only parameter in the model. It is assumed that this *d* parameter will depend mostly on the molecular details of the radical and to a lesser extend on the structure of the solute molecule. If the model is valid, then it should give a consistent description for a systematic variation of the composition (toluene concentration in CO_2), temperature and/or pressure using a fixed value for *d*. From the raw data in Fig. 5(b) it is clear that the increase in relaxation rate for methyl hydrogens per mole TEMPO is lower than for CH ring hydrogens. As the translational motion is the same, this indicates a slightly bigger effective interaction distance *d* for methyl hydrogens, possibly due to steric hindering. It is also possible that rotational modulation of the dipolar interaction gives an additional relaxation channel. However, this would lead to an increase in relaxation opposite to what is observed.

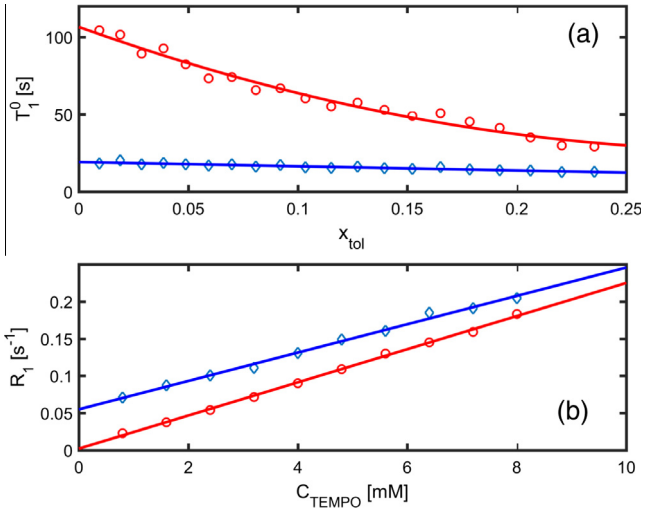

Fig. 5. (a) T_1^0 of the methyl (blue diamonds) and the ring (red circles) hydrogens of toluene as a function of the toluene mole fraction. (107 ± 3 bar, 18.0 ± 0.5 °C). (b) Longitudinal relaxation rate of the methyl (blue) and ring (red) hydrogens of toluene as a function of radical concentration in a mixture of 3.8 mol% toluene in CO_2. Solid lines are polynomial fits to guide the eye. (For interpretation of the references to color in this figure legend, the reader is referred to the web version of this article.)

In order to evaluate the radical induced relaxation rates for CO_2–toluene mixtures with different diffusion constants, toluene samples containing 100 mM, 50 mM and 25 mM TEMPO radical were mixed with CO_2 in various ratios (107 ± 3 bar, 18.0 ± 0.5 °C). The relaxation rates of these mixtures were again determined using a saturation recovery pulse sequence. The paramagnetic relaxivity, or increase in relaxation rate per molar TEMPO radical, is shown in Fig. 6 as a function of the molar ratio toluene to CO_2. In a qualitative sense it is clear that paramagnetic relaxation decreases for lower toluene content, indicating faster dynamics.

Using the diffusion constants as described by the fit in Fig. 4, it is possible to predict the relaxivity. The solid lines in Fig. 6(a) are the theoretical predictions using a distance of closest approach d = 0.234 nm for CH and d = 0.255 nm for CH_3. The error in the distance parameter is estimated at approximately 0.005 nm. For more details on the equations used in this analysis, see [5] and

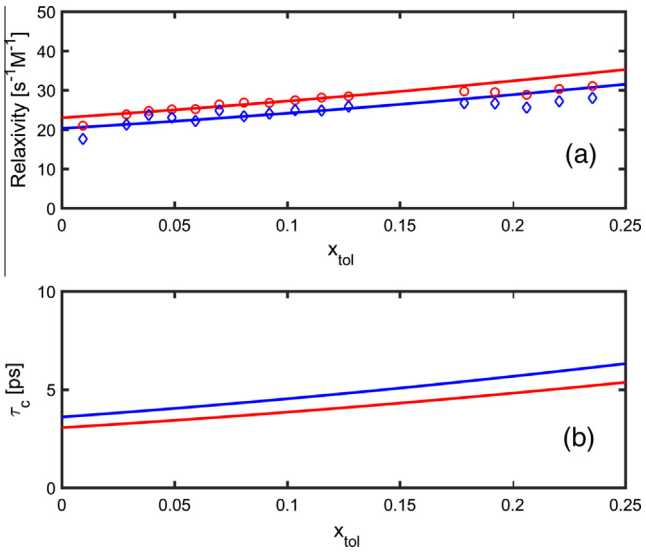

Fig. 6. (a) Increase in toluene relaxation rate per M TEMPO as a function of toluene molar fraction in the CO_2–toluene mixture. Blue symbols (diamonds) refer to CH_3 and red symbols (circles) to CH hydrogens. The solid lines are predictions from the Overhauser model for a distance of closest approach with TEMPO radicals $d = 0.234$ nm for CH and $d = 0.255$ nm for CH_3, using the diffusion constants as given by the solid line in Fig. 4. (b) The corresponding correlation times τ_c. (For interpretation of the references to color in this figure legend, the reader is referred to the web version of this article.)

references therein. In general, the agreement is quite satisfactory. At higher concentrations, the prediction weakly overestimates the experimental relaxivity, which may indicate stronger intermolecular interactions of the toluene molecules, leading to larger effective values for d. Note that in this analysis, the TEMPO diffusion constants in CO_2 are assumed to scale with the same factor as the toluene diffusion constants.

The distance parameters values happen to be very close to previous measurements for water–TEMPOL and ethanol–TEMPOL, where we found a value $d = 0.25$ nm. This confirms both that the truncation in the FFHS model to a fixed minimum distance seems valid and the interaction of TEMPO and TEMPOL radicals with accessible hydrogens in the probe molecule is independent of the solvent. Also, the quantitative scaling with the experimental diffusion constants confirms the dominant translational modulation of the dipolar interaction. It is not clear whether methyl rotations play an additional role in the dynamics, but most likely this contribution is small. In Fig. 6(b) we have plotted the correlation times corresponding with the predictions in Fig. 6(a). In the low concentration regime, we find typical correlation times between 3 and 4 ps, depending on the type of hydrogen (CH or CH_3). This should be compared with typical values of 25 ps for water at room temperature or 6 ps for water near the boiling point. This illustrates that the dynamics for toluene in CO_2 is indeed faster, even at the relatively low temperature of 20 °C, where the solvent is still in the liquid (sub-critical) phase.

The radical induced relaxation experiment was repeated at three temperatures (18, 23 and 32 °C) for a number of toluene concentrations. A similar analysis as shown above confirms that at the highest temperature (32 °C), the mobility increases and the low concentration correlation times decrease to about 2 resp. 3 ps for CH and CH_3 hydrogens in toluene at the used pressure of 107 bar. Further investigations of the full supercritical phase diagram are needed to explore the ultra fast regime, but based on tabulated viscosity data one expects that correlation times down to 1 ps or below are feasible. In this regime, the spectral density function predicts potential Overhauser enhancements for the full range of common NMR magnetic fields.

Using the determined distance of closest approach and diffusion coefficients, the Overhauser enhancements at infinite microwave power ($s = 1$) can be predicted with no adjustable parameters. For typical solvents like pure toluene or water near room temperature, the enhancement levels decrease from about −50 at 3.4 T to −10 and −5 at 9.4 and 14.1 T. Near the boiling point of water this increases to about −160 resp −70 and −30 at these magnetic field values. Note that the predictions for boiling water are actually quite close to the experimental observations [5,6], and translational motion seems to be sufficiently fast to account for the rather unexpected results at high temperatures. On the other hand, for supercritical media, such as CO_2 at a temperature of 32 °C and a toluene content below 5 mol%, the predicted enhancement increases to about −250 −180 and −140 at 3.4, 9.4 and 14.1 T. Note that in the limit for very low concentration or higher temperature/lower pressure, the enhancements are predicted to increase even further.

3.3. ODNP enhancements at 3.4 T

To test this prediction, preliminary DNP experiments have been performed at 3.4 T. As an extension to the supercritical CO_2 solvent, high pressure Overhauser DNP experiments have also been performed on a 50 mM TEMPOL water solution at 150 bar. Previous measurements [5] indicated a maximum enhancement of about −165, which is reached near the boiling point of water at ambient pressures. In the present setup it is possible to go to high pressure–high temperature conditions, where the mobility further increases. As in previous measurement, the radical EPR transition can be saturated at microwave powers below 1 W. With a further increase of microwave power, the main effect is a dielectric heating leading to faster dynamics and higher enhancements at the higher temperature [5,34]. The temperature of the sample can be determined from the shift in the water resonance [35]. The enhancement as a function of sample temperature is shown in Fig. 7. Here, the enhancement at elevated temperature is determined from the DNP enhanced signal intensity at a given microwave power (sample

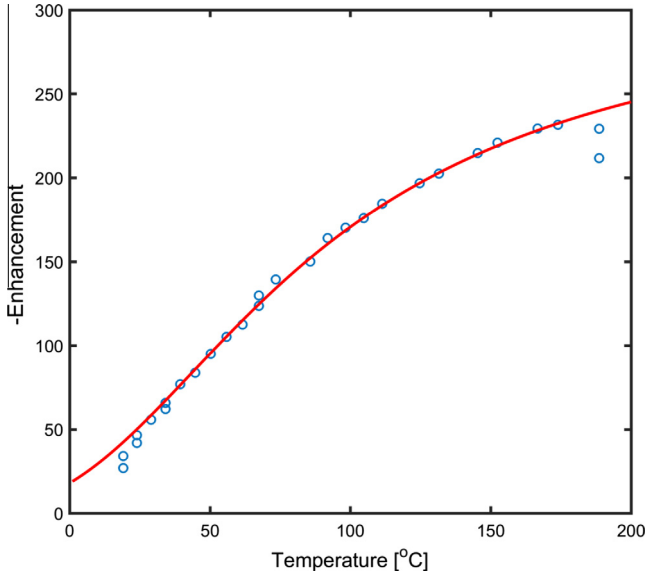

Fig. 7. Blue symbols: Overhauser enhancement at 3.4 T for 50 mM TEMPOL in high pressure water (150 bar) as a function of temperature. The solid red curve is a prediction from theory using a minimum distance parameter $d = 2.45$ Å and the self-diffusion coefficient and density as determined in literature. (For interpretation of the references to color in this figure legend, the reader is referred to the web version of this article.)

temperature), normalized to the room temperature thermal polarization signal and corrected for the temperature-dependent density [36] and for the temperature-dependent (electron) Boltzmann factor. The predicted enhancement for a minimum distance $d = 2.45$ Å and using the literature values for the self-diffusion constant for water as a function of temperature [5], is given by the solid curve in Fig. 7. This shows that by increasing the temperature to above 100 °C the Overhauser enhancements can indeed approach the theoretical maximum of −330. The critical temperature for water is 374 °C, so for the present experiment water is still in the subcritical regime.

To test the potential of ODNP in supercritical solvents, a preliminary experiment was performed with a 50 mM TEMPO in a 1:1 toluene–CO_2 mixture at 107 bar. This rather high toluene content was chosen to facilitate a reliable thermal equilibrium reference for the rather small detection volume of about 50 nl. The downside is that the molecular mobility is in-between that of liquid toluene and high pressure CO_2. Certainly, we are not in the supercritical regime and at the experimental temperature close to room temperature we remain in the liquid phase. Also, for the present mixture, we do not yet have the detailed reference data about diffusion constants and density as function of temperature. Although the dielectric losses in this mixture will be much smaller than for water, we cannot avoid microwave induced sample heating. In the absence of a suitable NMR temperature measurement for the present mixture, we cannot expect to be able to obtain a quantitative comparison with theory. For the present resonator geometry with an NMR detection coil inside the miniaturized nonradiative design it is also not trivial to separate the local intra-cavity signals from the extra-cavity signals in parts of the sample capillary outside the microwave field but within range of the NMR coil. However, it is still useful to test the setup and verify the protocols to create the sample with the appropriate concentration of radicals, move the sample plug to the microwave resonator and study the DNP effect in a qualitative sense. The results are represented by the symbols in Fig. 8, where we have plotted the increase in integrated signal intensity, normalized to the signal intensity of the sample for thermal polarization at room temperature, versus the applied microwave power. A calculation of the experimental DNP enhancement is not possible as the temperature, and thus the hydrogen density and Boltzmann population is not known. However, it is clear that the enhancement levels are at least comparable to that of high temperature water samples, as expected from the diffusion constant at room temperature as shown in Fig. 4. Future work, aiming at higher magnetic fields and higher microwave frequencies awaits the completion of suitable probes with efficient microwave resonators before a full quantitative test of the Overhauser dynamics in supercritical solvents is possible.

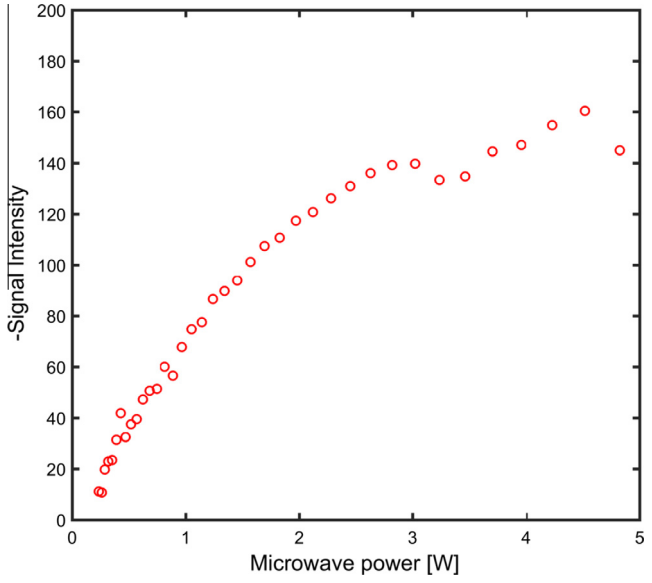

Fig. 8. Red symbols: Normalized integrated ^{1}H signal intensities at 3.4 T for 50 mM TEMPO in a 1:1 toluene–CO_2 mixture (107 bar, 18 °C), as function of the applied microwave power. (For interpretation of the references to color in this figure legend, the reader is referred to the web version of this article.)

4. Summary and conclusions

We have introduced a novel method of capillary flow NMR, coupled to a supercritical chromatography instrument that allows flexible determination of the Overhauser dynamics in toluene–CO_2 mixtures. The diffusion constant of toluene in such mixtures is measured in situ using a B_1 gradient NMR method. The longitudinal relaxation as function of radical concentration, toluene content and temperature, is measured and analyzed within the framework of the force-free hard sphere (FFHS) model for Overhauser cross-relaxation. This confirms that for toluene–CO_2 mixtures with a molar ratio less than 20%, the relaxation dynamics is well described with a single parameter for the minimum interaction distance $d = 2.34$ Å for the ring hydrogens and $d = 2.55$ Å for the methyl hydrogens. DNP enhancement experiments on high pressure superheated water are in good agreement with the model, and the interaction distance for water–TEMPOL molecules is essentially the same as for toluene–TEMPO. Preliminary measurements of the DNP enhancement for a toluene–CO_2 mixture confirm the potential enhancement for future work in supercritical solvents. For future applications in liquid state NMR enhanced by in situ Overhauser DNP, the implications are quite promising. First, the intrinsic longitudinal relaxation times can be quite long and double-quantum cross-relaxation can be dominant even at rather low radical concentrations, avoiding compromises in spectral resolution. Second, the measured correlation times in the range of 2–4 ps allow an extension to higher magnetic fields, potentially up to 14 T (600 MHz). Third, the capillary flow hyphenation with supercritical chromatography allows for a natural extension with automated sample handling and high sensitivity NMR analysis. Fourth, the increased mobility in supercritical solvents extends the molecular size range where Overhauser DNP can be effective. In particular, the high mobility of small stable radicals such as TEMPO in these solvents may provide efficient polarization transfer even for large molecular assemblies or biomolecules. A final advantage of supercritical solvents such as CO_2 is that the dielectric heating by microwaves is reduced in comparison to for example water, and potential microwave resonators can have a larger active volume.

More work is needed to extend the experiments into the full supercritical regime and to demonstrate the applicability at high magnetic fields.

Acknowledgements

This work is part of the UltraSense NMR project jointly funded by the European Union (EFRO), Gelderland and Overijssel (GO) and Radboud University. The authors would like to thank Gerrit Janssen and Hans Janssen for the technical support provided.

References

[1] A. Overhauser, Phys. Rev. 92 (1953) 411–415.
[2] T. Carver, C. Slichter, Phys. Rev. 92 (1953) 212–213.
[3] A. Abragam, Phys. Rev. 98 (1955) 1729–1735.
[4] M.-T. Türke, M. Bennati, Appl. Magn. Reson. 43 (2012) 129–138.

[5] P.J.M. van Bentum, G.H.A. van der Heijden, J.A. Villanueva-Garibay, A.P.M. Kentgens, Phys. Chem. Chem. Phys. 13 (2011) 17831–17840.
[6] V. Denysenkov, M.J. Prandolini, M. Gafurov, D. Sezer, B. Endeward, T.F. Prisner, Phys. Chem. Chem. Phys. 12 (2010) 5786–5790.
[7] P. Neugebauer, J.G. Krummenacker, V.P. Denysenkov, G. Parigi, C. Luchinat, T.F. Prisner, Phys. Chem. Chem. Phys. 15 (2013) 6049–6056.
[8] M. Reese, D. Lennartz, T. Marquardsen, P. Höfer, A. Tavernier, P. Carl, T. Schippmann, M. Bennati, T. Carlomagno, F. Engelke, C. Griesinger, Appl. Magn. Reson. 34 (2008) 301–311.
[9] M. Reese, M.-T. Türke, I. Tkach, G. Parigi, C. Luchinat, T. Marquardsen, A. Tavernier, P. Höfer, F. Engelke, C. Griesinger, M. Bennati, J. Am. Chem. Soc. 131 (2009) 15086–15087.
[10] A. Krahn, P. Lottmann, T. Marquardsen, A. Tavernier, M.-T. Türke, M. Reese, A. Leonov, M. Bennati, P. Hoefer, F. Engelke, C. Griesinger, Phys. Chem. Chem. Phys. 12 (2010) 5830–5840.
[11] J.H. Ardenkjaer-Larsen, B. Fridlund, A. Gram, G. Hansson, L. Hansson, M.H. Lerche, R. Servin, M. Thaning, K. Golman, Proc. Natl. Acad. Sci. USA 100 (2003) 10158–10163.
[12] M. Sharma, G. Janssen, J. Leggett, A. Kentgens, P. van Bentum, J. Magn. Reson. 258 (2015) 40–48.
[13] G.H.A. van der Heijden, A.P.M. Kentgens, P.J.M. van Bentum, Phys. Chem. Chem. Phys. 16 (2014) 8493–8502.
[14] L.A. Allen, T.E. Glass, H.C. Dorn, Anal. Chem. 60 (1988) 390–394.
[15] C.R. Yonker, J.C. Linehan, Prog. Nucl. Magn. Reson. Spectrosc. 47 (2005) 95–109.
[16] S. Gaemers, C.J. Elsevier, Chem. Soc. Rev. 28 (1999) 135–141.
[17] K. Albert, J. Chromatogr. A 785 (1997) 65–83.
[18] X. Wang, W.C. Isley III, S.I. Salido, Z. Sun, L. Song, K.H. Tsai, C.J. Cramer, H.C. Dorn, Chem. Sci. 6 (2015) 6482–6495.
[19] M.C.D. Tayler, S.B.G.J. van Meerten, A.P.M. Kentgens, P.J.M. van Bentum, Analyst 140 (2015) 6217–6221.
[20] I. Solomon, Phys. Rev. 99 (1955) 559–565.
[21] L.-P. Hwang, J.H. Freed, J. Chem. Phys. 63 (1975) 4017.
[22] J.M. Walsh, G.D. Ikonomou, M.D. Donohue, Fluid Phase Equilib. 33 (1987) 295–314.
[23] M.P. Ekart, K.L. Bennett, S.M. Ekart, G.S. Gurdial, C.L. Liotta, C.a. Eckert, AIChE J. 39 (1993) 235–248.
[24] P.J.M. van Bentum, J.W.G. Janssen, a.P.M. Kentgens, J. Bart, J.G.E. Gardeniers, J. Magn. Reson. 189 (2007) 104–113.
[25] G.S. Karczmar, D.B. Tweig, T.J. Lawry, G.B. Matson, M.W. Weiner, Magn. Reson. Med. 7 (1988) 111–116.
[26] K.C. Tijssen, J. Bart, R.M. Tiggelaar, J.H. Janssen, A.P. Kentgens, P.J.M. van Bentum, J. Magn. Reson. 263 (2016) 136–146.
[27] J.E. Tanner, J. Chem. Phys. 52 (1970) 2523.
[28] G. Annino, J. Villanueva-Garibay, P.J.M. van Bentum, A.A.K. Klaassen, A.P.M. Kentgens, Appl. Magn. Reson. 37 (2009) 851–864.
[29] R.L. Donkers, D.G. Leaist, J. Phys. Chem. B 101 (1997) 304–308.
[30] F.J.V. Santos, J. Phys. Chem. Ref. Data 35 (2006) 1.
[31] C.R. Wilke, P. Chang, AIChE J. 1 (1955) 264–270.
[32] K.R. Harris, J.J. Alexander, T. Goscinska, R. Malhotra, L.A. Woolf, J.H. Dymond, Mol. Phys. 78 (2006) 235–248.
[33] J.J. Suarez, J.L. Bueno, I. Medina, Chem. Eng. Sci. 48 (1993) 2419–2427.
[34] P. Neugebauer, J.G. Krummenacker, V.P. Denysenkov, C. Helmling, C. Luchinat, G. Parigi, T.F. Prisner, Phys. Chem. Chem. Phys. 16 (2014) 18781–18787.
[35] M.M. Hoffmann, M.S. Conradi, J. Am. Chem. Soc. 119 (1997) 3811–3817.
[36] W. Wagner, A. Pruss, J. Phys. Chem. Ref. Data 31 (2002) 387–535.